

EVALUATION OF INNER PRODUCTS OF IMPLICITLY-DEFINED FINITE ELEMENT FUNCTIONS ON MULTIPLY CONNECTED PLANAR MESH CELLS

JEFFREY S. OVALL AND SAMUEL E. REYNOLDS

ABSTRACT. Recent advancements in finite element methods allows for the implementation of mesh cells with curved edges. In the present work, we develop the tools necessary to employ multiply connected mesh cells, i.e. cells with holes, in planar domains. Our focus is efficient evaluation the H^1 semi-inner product and L^2 inner product of implicitly-defined finite element functions of the type arising in boundary element based finite element methods (BEM-FEM) and virtual element methods (VEM). These functions may be defined by specifying a polynomial Laplacian and a continuous Dirichlet trace. We demonstrate that these volumetric integrals can be reduced to integrals along the boundaries of mesh cells, thereby avoiding the need to perform any computations in cell interiors. The dominating cost of this reduction is solving a relatively small Nyström system to obtain a Dirichlet-to-Neumann map, as well as the solution of two more Nyström systems to obtain an “anti-Laplacian” of a harmonic function, which is used for computing the L^2 inner product. We demonstrate that high-order accuracy can be achieved with several numerical examples.

1. INTRODUCTION

Let $K \subset \mathbb{R}^2$ be an open, bounded, and connected planar region with a piecewise C^2 smooth boundary ∂K . Assume the boundary ∂K is partitioned into a finite number of *edges*, with each edge being C^2 smooth and connected. Edges are permitted to meet at interior angles strictly between 0 and 2π , so that ∂K has no cusps or slits. Consider the problem of computing the H^1 semi-inner product and L^2 inner product

$$(1) \quad \int_K \nabla v \cdot \nabla w \, dx ,$$

$$(2) \quad \int_K v w \, dx ,$$

where v, w are implicitly defined elements of a *local Poisson space* $V_p(K)$, which we define as follows. Fix a natural number p , and let $V_p(K)$ consist of the functions $v \in H^1(K) \cap C^2(K)$ such that:

- (a) for $p = 1$, v is harmonic in K ;
- (b) for $p \geq 2$, the Laplacian Δv is a polynomial of degree at most $p - 2$ in K ;
- (c) the trace $v|_{\partial K}$ is continuous;
- (d) the trace $v|_e$ along any edge $e \subset \partial K$ is the trace of a polynomial of degree at most p (defined over all of \mathbb{R}^2).

Note, for instance, that $V_p(K)$ contains all of the polynomials of degree at most p . Such subspaces of $H^1(K)$ arise naturally in the context of finite element methods posed over *curvilinear meshes*, whose mesh cells have curved edges. Our present interest is extending the application of these spaces to curvilinear meshes with *punctured* (i.e. multiply connected) mesh cells; see Figure 1.

Such spaces of implicitly-defined functions, whether arising from curvilinear, polygonal, or more conventional tetrahedral meshes, have appeared in the literature frequently in the last several years. Many readers are likely to be familiar with Virtual Element Methods (VEM), which have gained significant popularity in the last decade and have a large body of recent publications [5, 7–9], some of which concern employing curvilinear mesh cells [1, 6, 11, 30]. Our approach is more closely aligned with Boundary Element Based Finite Element Methods (BEM-FEM) and Trefftz methods [10, 15–18, 24–29]. In contrast to VEM, we actually construct a basis of $V_p(K)$ and do not require projections and so-called stabilization terms. Furthermore, while all

Date: March 13, 2023.

This work was partially supported by the National Science Foundation through NSF grant DMS-2012285 and NSF RTG grant DMS-2136228.

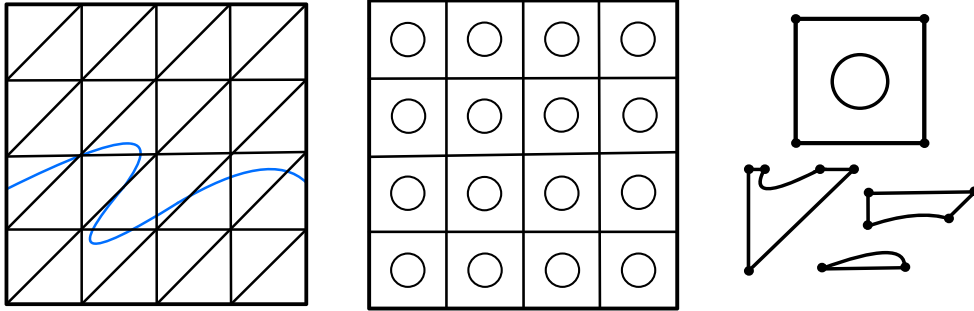


FIGURE 1. Left: A curvilinear mesh of a square domain featuring a curvilinear interface. Center: A curvilinear mesh of a square domain with circular punctures. Right: A few of the cells found in these meshes.

computations needed for forming the finite element system do not involve any calculations on the interior of mesh cells, and despite these basis functions being implicitly-defined, we have the option of obtaining information about the interior values, gradient, and higher derivatives of basis functions on the interior of each cell, and therefore those of the finite element solution. The basic framework for our approach was proposed in [2], where we proposed methods for construction of a basis that automatically preserves H^1 conformity, and proved estimates for associated interpolation operators. Subsequently, in [23], we demonstrated that practical computation of H^1 semi-inner products and L^2 inner products of functions in $V_p(K)$ are feasible whenever K is simply connected (i.e. has no holes). Indeed, we showed that these volumetric integrals can be reduced to boundary integrals, thereby circumventing any need to develop 2D quadratures for the unconventional geometries present in curvilinear meshes. The goal of this work is to extend these results to the case where K is multiply connected.

In Section 2, we briefly summarize how (1) and (2) may be computed in the case when K is simply connected. In Section 3, we address how these calculations can be modified in order to accommodate multiply connected mesh cells. We provide a handful of numerical illustrations in Section 4, and conclude in Section 5.

2. SIMPLY CONNECTED MESH CELLS

Let K be simply connected, and suppose that $v, w \in V_p(K)$. The goal of this section is to provide an overview of some of the techniques used to compute the integrals (1) and (2). In particular, we will see that each of these volumetric integrals can be feasibly reduced to boundary integrals over ∂K . These were discussed in detail in [23], although since its publication we have made some improvements that reduce computational cost, which we present here.

2.1. The H^1 Semi-inner Product. Given $v, w \in V_p(K)$, note that Δv and Δw are given polynomials of degree at most $p - 2$. Let P and Q be polynomials of degree at most p satisfying

$$\Delta(v - P) = 0, \quad \Delta(w - Q) = 0.$$

As pointed out in [19], such polynomials P and Q can be explicitly constructed term-by-term by observing that

$$(3) \quad P_\alpha(x) = \frac{|x|^2}{4(|\alpha| + 1)!} \sum_{k=0}^{\lfloor |\alpha|/2 \rfloor} \frac{(-1)^k (|\alpha| - k)!}{(k + 1)!} \left(\frac{|x|^2}{4} \right)^k \Delta^k(x^\alpha)$$

is a polynomial anti-Laplacian of x^α for a multi-index α . That is, $\Delta P_\alpha(x) = x^\alpha$. Note that, in practice, P_α is obtained only by manipulation of polynomial coefficients, and poses no computational barrier. The same can be said of other operations involving polynomials, such as gradients, etc.

Since the functions

$$\phi = v - P, \quad \psi = w - Q$$

are harmonic, we have the expansion

$$(4) \quad \begin{aligned} \int_K \nabla v \cdot \nabla w \, dx &= \int_K \nabla \phi \cdot \nabla w \, dx + \int_K \nabla P \cdot \nabla \psi \, dx + \int_K \nabla P \cdot \nabla Q \, dx \\ &= \int_{\partial K} w \frac{\partial \phi}{\partial \mathbf{n}} \, ds + \int_{\partial K} P \frac{\partial \psi}{\partial \mathbf{n}} \, ds + \int_K \nabla P \cdot \nabla Q \, dx . \end{aligned}$$

For the first two integrals in the final expression, the normal derivatives $\partial\phi/\partial\mathbf{n}$ and $\partial\psi/\partial\mathbf{n}$ may be computed using the Dirichlet-to-Neumann map discussed below. Furthermore, $\nabla P \cdot \nabla Q$ is clearly a polynomial of degree at most $2p - 2$. As noted in [3], a straightforward application of the Divergence Theorem shows that

$$(5) \quad \int_K x^\alpha \, dx = \frac{1}{2 + |\alpha|} \int_{\partial K} (x \cdot \mathbf{n}) x^\alpha \, ds .$$

In this fashion, we reduce the volumetric integral $\int_K \nabla v \cdot \nabla w \, dx$ to readily computable boundary integrals.

2.2. A Dirichlet-to-Neumann Map. Consider the problem of determining the normal derivative of a harmonic function ϕ given its Dirichlet trace $\phi|_{\partial K}$. Recall that $\widehat{\phi}$ is a harmonic conjugate of a harmonic function ϕ whenever $\phi, \widehat{\phi}$ are continuously twice differentiable on K and satisfy the Cauchy-Riemann equations:

$$\frac{\partial \phi}{\partial x_1} = \frac{\partial \widehat{\phi}}{\partial x_2} , \quad \frac{\partial \phi}{\partial x_2} = -\frac{\partial \widehat{\phi}}{\partial x_1} .$$

Given that ϕ is harmonic on a simply connected domain K , the existence of a harmonic conjugate of ϕ is guaranteed, and $\widehat{\phi}$ is unique up to an additive constant. If ∂K is smooth, for every $x \in \partial K$ it holds that

$$(6) \quad \frac{1}{2} \widehat{\phi}(x) + \int_{\partial K} \frac{\partial G(x, y)}{\partial \mathbf{n}(y)} \widehat{\phi}(y) \, dS(y) = \int_{\partial K} G(x, y) \frac{\partial \widehat{\phi}}{\partial \mathbf{n}}(y) \, dS(y)$$

where $G(x, y) = -(2\pi)^{-1} \ln|x - y|$ is the fundamental solution of the Laplacian in \mathbb{R}^2 . Supposing that the boundary ∂K is traversed counterclockwise, we let \mathbf{t} denote the unit tangent vector and \mathbf{n} denote the outward unit normal vector, so that the normal and tangential derivatives of ϕ and $\widehat{\phi}$ are related by

$$(7) \quad \frac{\partial \phi}{\partial \mathbf{n}} = \frac{\partial \widehat{\phi}}{\partial \mathbf{t}} , \quad \frac{\partial \widehat{\phi}}{\partial \mathbf{n}} = -\frac{\partial \phi}{\partial \mathbf{t}} ,$$

from which the right-hand side in (6) can be computed. Since $\widehat{\phi}$ is unique only up to an additive constant, we impose $\int_K \widehat{\phi} \, ds = 0$, which we add to the left-hand side above to obtain

$$(8) \quad \frac{1}{2} \widehat{\phi}(x) + \int_{\partial K} \left(\frac{\partial G(x, y)}{\partial \mathbf{n}(y)} + 1 \right) \widehat{\phi}(y) \, dS(y) = - \int_{\partial K} G(x, y) \frac{\partial \phi}{\partial \mathbf{t}}(y) \, dS(y) .$$

In practice, we solve this integral equation numerically for $\widehat{\phi}$ on ∂K using a Nyström method, where the right-hand side is computed using the tangential derivative of ϕ , which is readily accessible from its trace $\phi|_{\partial K}$. Having obtained values of the harmonic conjugate $\widehat{\phi}$ on the boundary ∂K , we may obtain its tangential derivative $\partial\widehat{\phi}/\partial\mathbf{t}$ via numerical differentiation, which then yields values of the normal derivative $\partial\phi/\partial\mathbf{n}$. Indeed, if $x(t)$ is a sufficiently smooth parameterization of ∂K and we define $G(t) = \widehat{\phi}(x(t))$, then

$$(9) \quad G'(t) = \frac{\partial \widehat{\phi}}{\partial \mathbf{t}}(x(t)) |x'(t)| = \frac{\partial \phi}{\partial \mathbf{n}}(x(t)) |x'(t)| .$$

Since $G(t)$ is periodic, a natural choice to obtain $G'(t)$ is to write a Fourier expansion $G(t) = \sum_{k=-\infty}^{\infty} \omega_k e^{ikt}$ and obtain an approximation of $G'(t)$ by truncating the series

$$(10) \quad G'(t) = \sum_{k=-\infty}^{\infty} ik\omega_k e^{ikt} .$$

In practice, a Fast Fourier Transform (FFT) may be used on a discretization of $G(t)$, and an inverse FFT used on the coefficients $ik\omega_k$ to obtain the approximate values of $G'(t)$.

Details of such calculations, including the case where ∂K has corners, are discussed in [22].

2.3. **The L^2 Inner Product.** Let $v = \phi + P$ and $w = \psi + Q$ be as above. We have the expansion

$$(11) \quad \int_K v w \, dx = \int_K \phi \psi \, dx + \int_K Q \phi \, dx + \int_K P \psi \, dx + \int_K P Q \, dx .$$

Notice that the last integral can be computed with (5), whereas the two middle integrals have the form

$$\int_K r \eta \, dx$$

where r is a polynomial and η is harmonic. Using (3), let R be a polynomial such that

$$\Delta R = r ,$$

then applying Green's Second Identity, we have

$$(12) \quad \int_K r \eta \, dx = \int_K \eta \Delta R \, dx = \int_{\partial K} \left[\eta \frac{\partial R}{\partial \mathbf{n}} - R \frac{\partial \eta}{\partial \mathbf{n}} \right] ds .$$

The remaining integral to be computed in (11) is the L^2 inner product of the two harmonic functions ϕ and ψ . Toward this end, suppose that Φ is an anti-Laplacian of the harmonic function ϕ , that is,

$$\Delta \Phi = \phi .$$

Then using Green's Second Identity again yields

$$(13) \quad \int_K \phi \psi \, dx = \int_K \psi \Delta \Phi \, dx = \int_{\partial K} \left[\psi \frac{\partial \Phi}{\partial \mathbf{n}} - \Phi \frac{\partial \psi}{\partial \mathbf{n}} \right] ds .$$

The problem of determining such a Φ , in particular its trace $\Phi|_{\partial K}$ and normal derivative $\partial \Phi / \partial \mathbf{n}$, is addressed as follows.

2.4. **Anti-Laplacians of Harmonic Functions.** Notice that if Φ is an anti-Laplacian of ϕ , it holds that Φ is *biharmonic*, that is, $\Delta^2 \Phi = 0$. A well-known fact (see, for example, pp. 269 of [12]) is that every biharmonic function is of the form

$$\Phi(x) = \operatorname{Re} [\bar{z}f(z) + g(z)] ,$$

where f, g are some analytic functions, $\operatorname{Re} [z]$ denotes the real part of $z \in \mathbb{C}$, \bar{z} denotes the complex conjugate, and we use the natural identification of the complex plane with \mathbb{R}^2 via $x = (x_1, x_2) \mapsto z = x_1 + ix_2$. Since any anti-Laplacian of ϕ will suffice for our purposes, we will take $g = 0$ and write

$$\Phi(x) = \frac{x_1 \rho(x) + x_2 \widehat{\rho}(x)}{4} ,$$

where $\rho = 4(\operatorname{Re} f)$ is a harmonic function and $\widehat{\rho} = 4(\operatorname{Im} f)$ is a harmonic conjugate of ρ . It follows from the Cauchy-Riemann equations that

$$\phi = \Delta \Phi = \frac{\partial \rho}{\partial x_1} = \frac{\partial \widehat{\rho}}{\partial x_2} ,$$

and that the gradients of ρ and $\widehat{\rho}$ must take the form

$$\nabla \rho = \begin{pmatrix} \phi \\ -\widehat{\phi} \end{pmatrix} , \quad \nabla \widehat{\rho} = \begin{pmatrix} \widehat{\phi} \\ \phi \end{pmatrix} ,$$

where $\widehat{\phi}$ is a harmonic conjugate of ϕ .

Remark 2.1. Note that the gradient of Φ is given by

$$\nabla \Phi(x) = \frac{1}{4} \begin{pmatrix} \rho(x) \\ \widehat{\rho}(x) \end{pmatrix} + \frac{1}{4} \begin{pmatrix} x_1 & x_2 \\ x_2 & -x_1 \end{pmatrix} \begin{pmatrix} \phi(x) \\ \widehat{\phi}(x) \end{pmatrix}$$

from which we may obtain the normal derivative $\partial \Phi / \partial \mathbf{n}$.

Remark 2.2. For any fixed constants a and b , we have that

$$\frac{x_1(\rho(x) + a) + x_2(\widehat{\rho}(x) + b)}{4}$$

is also an anti-Laplacian of ϕ , since $(ax_1 + bx_2)/4$ is harmonic.

In order to compute ρ and $\widehat{\rho}$, consider the following. For the sake of illustration, we assume that the boundary ∂K is smooth, but a similar approach works when ∂K is only piecewise smooth, using some minor modifications. Given the traces of ϕ and $\widehat{\phi}$ on ∂K , we have access to the tangential derivative of ρ via

$$\frac{\partial \rho}{\partial \mathbf{t}} = \begin{pmatrix} \phi \\ -\widehat{\phi} \end{pmatrix} \cdot \mathbf{t}.$$

Given a sufficiently smooth parameterization $x(t) : [0, 2\pi] \rightarrow \partial K$ of the boundary, we define $g : [0, 2\pi] \rightarrow \mathbb{R}$ by

$$g(t) = \frac{\partial \rho}{\partial \mathbf{t}}(x(t)) |x'(t)|.$$

By the Fundamental Theorem of Calculus, we may obtain an anti-derivative G via

$$G(t) = \int_0^t g(\tau) d\tau = \int_0^t \nabla \rho(x(\tau)) \cdot x'(\tau) d\tau = \rho(x(t)).$$

Note that g is 2π -periodic and admits a Fourier expansion

$$g(t) = \sum_{k=-\infty}^{\infty} \omega_k e^{ikt}.$$

As mentioned above, in practice we truncate this series and compute the Fourier coefficients ω_k using an FFT. Integrating termwise yields

$$\rho(x(t)) = G(t) = C + \omega_0 t + \sum_{\substack{k=-\infty \\ k \neq 0}}^{\infty} \frac{\omega_k}{ik} e^{ikt}$$

for an arbitrary constant C . In light of Remark 2.2, we may pick C arbitrarily; for instance, choose $C = 0$. Moreover, since $\rho(x(t))$ is 2π -periodic, we also see that $\omega_0 = 0$. In the computational context, we apply an inverse FFT to the coefficients $-\mathrm{i}\omega_k/k$ in order to obtain approximate values of ρ on the boundary. We apply an analogous procedure to obtain values of $\widehat{\rho}$ on the boundary, using the tangential derivative data

$$\frac{\partial \widehat{\rho}}{\partial \mathbf{t}} = \begin{pmatrix} \widehat{\phi} \\ \phi \end{pmatrix} \cdot \mathbf{t}$$

and computing an anti-derivative of

$$\widehat{g}(t) = \frac{\partial \widehat{\rho}}{\partial \mathbf{t}}(x(t)) |x'(t)|.$$

2.5. Piecewise Smooth Boundaries. In our discussion so far, we have assumed the cell boundary ∂K to be smooth, but here we will briefly address how the calculations described above can be modified when ∂K has one or more corners. Elaboration on these modifications can be found in [22].

Each edge of the mesh cell K is discretized into $2n+1$ points, including the endpoints, so that the boundary is discretized into $N = 2n \times (\# \text{ edges of } K)$ points, with redundant endpoints being neglected. When an edge $e \subseteq \partial K$ is a C^2 smooth closed contour, the boundary points are assumed to be sampled according a *strongly regular parameterization* $x(t)$ of e (i.e. $|x'(t)| \geq \delta$ for all $x(t) \in e$ and for some fixed $\delta > 0$). In the case where e terminates at a corner, we employ a *Kress reparameterization*, defined as follows (cf. [20]). Suppose that $x(t)$ is a strongly regular parameterization of e for $t \in [0, 2\pi]$, then define $\tilde{x}(u) = x(\tau(u))$ using

$$\tau(u) = \frac{2\pi[c(u)]^\sigma}{[c(u)]^\sigma + [1-c(u)]^\sigma}, \quad c(u) = \left(\frac{1}{2} - \frac{1}{\sigma}\right) \left(\frac{u}{\pi} - 1\right)^2 + \frac{1}{\sigma} \left(\frac{u}{\pi} - 1\right) + \frac{1}{2}, \quad u \in [0, 2\pi]$$

where the *Kress parameter* $\sigma \geq 2$ is fixed. The Kress reparameterization is not regular, with $\tilde{x}'(u)$ vanishing at the endpoints. Indeed, $\tau'(u)$ has roots at 0 and 2π of order $\sigma - 1$, which leads to heavy sampling of the boundary near corners. This effect is amplified for larger values of σ .

Recall that whenever η has a sufficiently smooth Dirichlet trace, we can compute the *weighted tangential derivative*

$$\frac{d}{dt} \eta(x(t)) = \frac{\partial \eta}{\partial \mathbf{t}}(x(t)) |x'(t)|$$

by using, for instance, the FFT-based approach described by (10). Replacing $x(t)$ with a Kress reparameterization leads to difficulty in recovering the values of the tangential derivative from the weighted tangential derivative. The same can be said for the *weighted normal derivative*

$$\frac{\partial \eta}{\partial \mathbf{n}}(x(t)) |x'(t)| .$$

Notice, though, that for the sake of computing the boundary integral

$$\int_{\partial K} \omega \frac{\partial \eta}{\partial \mathbf{n}} ds = \int_{t_0}^{t_f} \omega(x(t)) \frac{\partial \eta}{\partial \mathbf{t}}(x(t)) |x'(t)| dt$$

the weighting term $|x'(t)|$ appears in the Jacobian anyway, so it is natural to keep the tangential and normal derivatives in their weighted form, including the case when using a Kress reparameterization.

Note that, for the sake of effectively applying an FFT, we assume that the parameter t is sampled at equispaced nodes $t_k = hk$, $h = \pi/n$, $0 \leq j \leq 2n + 1$, and likewise for the parameter u when using a Kress reparameterization.

2.6. Summary of Simply Connected Case. Thus far, we have all the necessary tools to compute the goal integrals (1) and (2) in the case where K is simply connected. It is worth reiterating that both of these volumetric integrals have been successfully reduced to contour integrals along the boundary ∂K , and there is no need for 2-dimensional quadratures as *all necessary computations occur only on ∂K* .

We have the option, though, of obtaining interior values of $v \in V_p(K)$ as follows. Write $v = \phi + P$ as above, and determine a harmonic conjugate $\hat{\phi}$ of ϕ . Then $f = \phi + i\hat{\phi}$ is an analytic function, and for any fixed interior point $z = x_1 + ix_2 \in K$ we have Cauchy's integral formula

$$(14) \quad f(z) = \frac{1}{2\pi i} \oint_{\partial K} \frac{f(\zeta)}{\zeta - z} d\zeta .$$

Furthermore, we can obtain interior values of $\nabla \phi$ by observing that

$$f' = \frac{\partial \phi}{\partial x_1} - i \frac{\partial \phi}{\partial x_2} , \quad f'(z) = \frac{1}{2\pi i} \oint_{\partial K} \frac{f(\zeta)}{(\zeta - z)^2} d\zeta .$$

Interior values of higher derivatives, such as the components of the Hessian, can be obtained in similar fashion if so desired.

We conclude this section with a few remarks about computational complexity. Assume the boundary ∂K is parameterized and then discretized using N points. The Nyström system resulting from (8) is dense, though well-conditioned, and simple linear solvers come with a computational cost $\mathcal{O}(N^3)$. Using more sophisticated methods, such as GMRES, make an improvement, but in general will never be better than $\mathcal{O}(N^2)$. Although even more sophisticated methods, such as those based on hierarchical matrices [14] or hierarchical semiseparable matrices [31], can reduce the computational complexity even further, for relatively small problems such as those considered here, GMRES is sufficient.

The FFT calls used for numerical differentiation have a computational cost of $\mathcal{O}(N \log N)$, and integration along ∂K using (using, say, the trapezoid rule) take $\mathcal{O}(N)$ operations. Operations on polynomials, such as computing anti-Laplacians, can be performed by manipulation of the coefficients and do not meaningfully contribute to the computational cost. So despite the many terms we have encountered in the expansion of the integrals (1) and (2), in practice these expansions are relatively cheap in comparison to the cost of obtaining the trace of the harmonic conjugate. Note that the latter computation need only happen once for each function $v \in V_p(K)$ considered.

Additionally, we can use the notion of trigonometric interpolation to reduce computational cost even further, as was explored in [22]. With the boundary discretized into N points, we can solve the the Nyström system obtained from (8) as usual to obtain the harmonic conjugate $\hat{\phi}$. While performing numerical differentiation with FFT as proposed, we have the Fourier coefficients at our disposal, which allows for rapid interpolation to, say, $M = 2^m N$ points. We then compute the boundary integrals obtained from expanding (1) and (2) using standard 1D quadratures (e.g. the trapezoid rule, Simpson's rule, etc.) on the larger collection of M points. The heuristics presented in [22] suggest that similar levels of accuracy are achieved as would be in the case where all M sampled points are used for solving the Nyström system.

In the next two sections, we address how our approach can be modified to accommodate multiply connected mesh cells.

3. PUNCTURED CELLS

We now consider the case with K being multiply connected. That is, we take $K_0, K_1, \dots, K_m \subset \mathbb{R}^2$ to be simply connected, open, bounded regions, such that:

- (a) for each $1 \leq j \leq m$, we have that \overline{K}_j is a proper subset of K_0 —that is, $\overline{K}_j \subset K_0$;
- (b) for each $1 \leq i < j \leq m$, the closures of K_i and K_j are disjoint—that is, $\overline{K}_i \cap \overline{K}_j = \emptyset$.

Additionally, we will require that for each $0 \leq j \leq m$, the boundary ∂K_j is piecewise C^2 smooth without slits or cusps. We then take K to be the region

$$K = K_0 \setminus \bigcup_{j=1}^m \overline{K}_j .$$

We refer to K_j as the j th *hole* (or *puncture*) of K . We sometimes call ∂K_0 the *outer boundary* of K , and ∂K_j the j th *inner boundary*. The outer boundary is assumed to be oriented counterclockwise, and the inner boundaries oriented clockwise, with the unit tangential vector \mathbf{t} , wherever it is defined, oriented accordingly. The outward unit normal \mathbf{n} is therefore always a $\pi/2$ clockwise rotation of \mathbf{t} .

In the simply connected case, we made liberal use of the notion of harmonic conjugates. However, in multiply connected domains, a given harmonic function is not guaranteed to have a harmonic conjugate, e.g. $\ln|x|$ on an annulus centered at the origin. The following theorem, which is proved in [4], for example, provides a very helpful characterization of which harmonic functions have a harmonic conjugate.

Theorem 3.1 (Logarithmic Conjugation Theorem). *For each of the m holes of a multiply connected domain K , fix a point $\xi_j \in K_j$. Suppose that ϕ is a harmonic function on K . Then there are real constants a_1, \dots, a_m such that, for each $x \in K$,*

$$\phi(x) = \psi(x) + \sum_{j=1}^m a_j \ln|x - \xi_j|$$

where ψ is the real part of an analytic function. In particular, ψ has a harmonic conjugate $\widehat{\psi}$.

To simplify the notation in what is to come, it will be convenient to define

$$(15) \quad \lambda_j(x) = \ln|x - \xi_j|, \quad x \in K, \quad 1 \leq j \leq m .$$

In a minor notational shift from Section 2, note that, in this section, we will reserve ψ to represent a “conjugable part” of a harmonic function ϕ , rather than treat ϕ and ψ as independent harmonic functions as we did in the previous section.

3.1. A Dirichlet-to-Neumann Map for Punctured Cells. Our present goal is to determine the coefficients a_1, \dots, a_m , as in the statement of Theorem 3.1, given the trace of a harmonic function ϕ . We will see that we simultaneously determine $\widehat{\psi}$ by solving an integral equation similar to (8), and thereby arrive at the Dirichlet-to-Neumann map

$$(16) \quad \phi|_{\partial K} \mapsto \frac{\partial \phi}{\partial \mathbf{n}} = \frac{\partial \widehat{\psi}}{\partial \mathbf{t}} + \sum_{j=1}^m a_j \frac{\partial \lambda_j}{\partial \mathbf{n}} .$$

Assume for now that the boundary ∂K is C^2 smooth. The case with corners is handled with Kress reparameterization, as discussed in the previous section. Our current task is to generalize the technique described by (8) in the case where K is multiply connected. An alternative approach to the method we discuss here is presented in [13], which is comparable to our method in terms of cost and accuracy when all boundary edges are smooth, but does not achieve similar levels of accuracy when corners are present.

Let $\widehat{\psi}$ denote a harmonic conjugate of ψ satisfying $\int_{\partial K} \widehat{\psi} ds = 0$. Just as in the simply connected case, we have

$$\frac{1}{2} \widehat{\psi}(x) + \int_{\partial K} \left(\frac{\partial G(x, y)}{\partial \mathbf{n}(y)} + 1 \right) \widehat{\psi}(y) dS(y) = \int_{\partial K} G(x, y) \frac{\partial \widehat{\psi}}{\partial \mathbf{n}}(y) dS(y) .$$

Making the replacement

$$\frac{\partial \widehat{\psi}}{\partial \mathbf{n}} = -\frac{\partial \psi}{\partial \mathbf{t}} = -\frac{\partial \phi}{\partial \mathbf{t}} + \sum_{j=1}^m a_j \frac{\partial \lambda_j}{\partial \mathbf{t}}$$

and rearranging yields

$$(17) \quad \begin{aligned} \frac{1}{2} \widehat{\psi}(x) + \int_{\partial K} \left(\frac{\partial G(x, y)}{\partial \mathbf{n}(y)} + 1 \right) \widehat{\psi}(y) dS(y) - \sum_{j=1}^m a_j \int_{\partial K} G(x, y) \frac{\partial \lambda_j}{\partial \mathbf{t}}(y) dS(y) \\ = - \int_{\partial K} G(x, y) \frac{\partial \phi}{\partial \mathbf{t}}(y) dS(y) . \end{aligned}$$

This integral equation is underdetermined due to the m additional degrees of freedom a_1, \dots, a_m in contrast to (8). To resolve this, we multiply both sides of $\phi = \psi + \sum_{j=1}^m a_j \lambda_j$ by the normal derivative $\partial \lambda_\ell / \partial \mathbf{n}$ and integrate over ∂K to obtain

$$\int_{\partial K} \phi \frac{\partial \lambda_\ell}{\partial \mathbf{n}} ds = \int_{\partial K} \psi \frac{\partial \lambda_\ell}{\partial \mathbf{n}} ds + \sum_{j=1}^m a_j \int_{\partial K} \lambda_j \frac{\partial \lambda_\ell}{\partial \mathbf{n}} ds .$$

Invoking Green's Second Identity and the Cauchy-Riemann equations yields

$$\int_{\partial K} \psi \frac{\partial \lambda_\ell}{\partial \mathbf{n}} ds = \int_{\partial K} \lambda_\ell \frac{\partial \psi}{\partial \mathbf{n}} ds = \int_{\partial K} \lambda_\ell \frac{\partial \widehat{\psi}}{\partial \mathbf{t}} ds .$$

To write this in a form more conducive to computation, observe that the Fundamental Theorem of Calculus for contour integrals implies that

$$\int_{\partial K} \frac{\partial(\widehat{\psi} \lambda_\ell)}{\partial \mathbf{t}} ds = 0$$

since ∂K consists of $m + 1$ closed contours. From the Product Rule, we obtain

$$\int_{\partial K} \lambda_\ell \frac{\partial \widehat{\psi}}{\partial \mathbf{t}} ds = - \int_{\partial K} \widehat{\psi} \frac{\partial \lambda_\ell}{\partial \mathbf{t}} ds .$$

Therefore, $\widehat{\psi}$ ought to satisfy

$$(18) \quad - \int_{\partial K} \widehat{\psi} \frac{\partial \lambda_\ell}{\partial \mathbf{t}} ds + \sum_{j=1}^m a_j \int_{\partial K} \lambda_j \frac{\partial \lambda_\ell}{\partial \mathbf{n}} ds = \int_{\partial K} \phi \frac{\partial \lambda_\ell}{\partial \mathbf{n}} ds , \quad 1 \leq \ell \leq m .$$

In summary, we have obtained a system of equations (17) and (18) for determining the trace of $\widehat{\psi}$ on ∂K . Discretizing the boundary into N points, as we did for the simply connected case, this system of equations yields a square augmented Nyström system in $N + m$ variables, which we may solve with the same techniques used for solving (8). The case when ∂K has corners can be handled using a Kress reparameterization, just as in the simply connected case.

3.2. Anti-Laplacians of Harmonic Functions on Punctured Cells. Next, we wish to construct an anti-Laplacian of a harmonic function

$$\phi = \psi + \sum_{j=1}^m a_j \lambda_j$$

as in the statement of Theorem 3.1. It is simple to verify that

$$\Lambda_j(x) = \frac{1}{4} |x - \xi_j|^2 (\ln |x - \xi_j| - 1)$$

is an anti-Laplacian of $\lambda_j(x) = \ln |x - \xi_j|$, so if Ψ is an anti-Laplacian of ψ , then we have that

$$(19) \quad \Phi = \Psi + \sum_{j=1}^m a_j \Lambda_j$$

is an anti-Laplacian of ϕ . The normal derivative can be computed using

$$\nabla\Phi = \nabla\Psi + \sum_{j=1}^m a_j \nabla\Lambda_j, \quad \nabla\Lambda_j(x) = \frac{1}{4}(2\ln|x - \xi_j| - 1)(x - \xi_j).$$

Analogous to the simply connected case, we might seek potentials $\rho, \hat{\rho}$ of the vector fields

$$\mathbf{F} = \begin{pmatrix} \psi \\ -\hat{\psi} \end{pmatrix}, \quad \hat{\mathbf{F}} = \begin{pmatrix} \hat{\psi} \\ \psi \end{pmatrix}.$$

While \mathbf{F} and $\hat{\mathbf{F}}$ both have vanishing curls, this is not sufficient to guarantee that they are both conservative on a multiply connected domain—a simple counterexample being

$$\psi(x) = \frac{x_1}{|x|^2}, \quad \hat{\psi}(x) = -\frac{x_2}{|x|^2},$$

taken on a circular annulus centered at the origin.

An elementary observation from complex analysis is that an analytic function $g = \psi + i\hat{\psi}$ has an antiderivative if and only if $\mathbf{F} = (\psi, -\hat{\psi})$ and $\hat{\mathbf{F}} = (\hat{\psi}, \psi)$ are conservative vector fields. Indeed, $G = \rho + i\hat{\rho}$ satisfies $G' = g$ for $\nabla\rho = \mathbf{F}$ and $\nabla\hat{\rho} = \hat{\mathbf{F}}$. This simple fact inspires us to decompose g as $g_0 + g_1$, where g_0 has an antiderivative and the real part of g_1 has an anti-Laplacian which can be computed a priori. The following proposition reveals such a decomposition. The proof is inspired by that given in [4] and is unlikely to surprise a reader familiar with elementary complex analysis, but we include it for the sake of completeness.

Proposition 3.2. *Let $g = \psi + i\hat{\psi}$ be analytic on a multiply connected domain K . Let $\zeta_j \in K_j$ denote a point fixed in the j th hole of K . Then there are complex constants $\alpha_j \in \mathbb{C}$ such that*

$$g(z) = g_0(z) + \sum_{j=1}^m \frac{\alpha_j}{z - \zeta_j},$$

where g_0 has an antiderivative.

Proof. For each $1 \leq j \leq m$, let

$$\alpha_j = -\frac{1}{2\pi i} \oint_{\partial K_j} g \, dz$$

where ∂K_j is the boundary of the j th hole traversed clockwise, and define

$$g_0(z) := g(z) - \sum_{j=1}^m \frac{\alpha_j}{z - \zeta_j}.$$

We wish to show that g_0 has an antiderivative, i.e. there is an analytic function G_0 for which $G_0' = g_0$. It will suffice to show that $\oint_{\gamma} g_0 \, dz = 0$ for any closed contour γ in K . To see why, fix any point $z_0 \in K$ and define

$$G_0(z) = \int_{\gamma(z_0, z)} g_0(\zeta) \, d\zeta$$

where $\gamma(z_0, z)$ is any contour starting at z_0 and terminating at $z \in K$. Since this integral would be path independent, it would hold that G_0 is well defined and $G_0' = g_0$.

Let γ be a closed contour in K . If γ is homotopic to a point, then

$$\oint_{\gamma} g_0 \, dz = \oint_{\gamma} g \, dz - \sum_{j=1}^m \oint_{\gamma} \frac{\alpha_j}{z - \zeta_j} \, dz = 0$$

holds because g and $(z - \zeta_j)^{-1}$ are analytic in simply connected open subset of K . If γ is homotopic to ∂K_ℓ , then by the Deformation Theorem we have

$$\begin{aligned} \oint_{\gamma} g_0 dz &= \oint_{\partial K_\ell} g_0 dz \\ &= \oint_{\partial K_\ell} g dz - \sum_{j=1}^m \oint_{\partial K_\ell} \frac{\alpha_j}{z - \zeta_j} dz \\ &= -2\pi i \alpha_\ell - \oint_{\partial K_\ell} \frac{\alpha_\ell}{z - \zeta_\ell} dz = 0. \end{aligned}$$

Note that the same conclusion holds when γ is oriented opposite to ∂K_j . Finally, if γ is any closed contour in K that is not homotopic to a point, it holds that γ can be decomposed as a closed chain (cf. Theorem 2.4 in [21])

$$\gamma \sim m_1 \gamma_{\ell_1} + \cdots + m_n \gamma_{\ell_n}, \quad n \leq m$$

with γ_{ℓ_j} being homotopic to ∂K_j and m_j being the winding number of γ with respect to ζ_j . Then

$$\oint_{\gamma} g_0 dz = \sum_{j=1}^n m_j \oint_{\gamma_{\ell_j}} g_0 dz = 0$$

holds by the previous conclusion. Therefore $\int_{\gamma} g_0 dz = 0$ for any closed contour in γ . As remarked above, this is sufficient to show that g_0 has an antiderivative. \square

Remark 3.3. For $\alpha_j = b_j + ic_j$ in the proof above, we have

$$(20) \quad b_j = -\frac{1}{2\pi} \int_{\partial K_j} (\widehat{\psi}, \psi) \cdot \mathbf{t} ds, \quad c_j = \frac{1}{2\pi} \int_{\partial K_j} (\psi, -\widehat{\psi}) \cdot \mathbf{t} ds$$

are real-valued contour integrals around the boundary of the j th hole. Again, note that the inner boundary ∂K_j is taken to be oriented clockwise, with \mathbf{t} behaving accordingly.

Using the above results, we may decompose $g = \psi + i\widehat{\psi}$ into one part that has an antiderivative

$$g_0 = \psi_0 + i\widehat{\psi}_0,$$

and another part that is a linear combination of rational functions

$$\sum_{j=1}^m \frac{\alpha_j}{z - \zeta_j} = \sum_{j=1}^m (b_j \mu_j - c_j \widehat{\mu}_j) + i \sum_{j=1}^m (c_j \mu_j + b_j \widehat{\mu}_j), \quad \begin{pmatrix} \mu_j \\ -\widehat{\mu}_j \end{pmatrix} = \nabla \ln |x - \xi_j|,$$

where we use $\zeta_j = \xi_j \cdot (1, i)$, with ξ_j being chosen when Theorem 3.1 is applied. Easy calculations verify that

$$M_j(x; b_j, c_j) = \frac{1}{2} (b_j, c_j) \cdot (x - \xi_j) \ln |x - \xi_j|$$

satisfies $\Delta M_j = b_j \mu_j - c_j \widehat{\mu}_j$, and whose normal derivative can be directly obtained from

$$\nabla M_j(x; b_j, c_j) = \frac{1}{2} (b_j \mu_j - c_j \widehat{\mu}_j) (x - \xi_j) + \frac{1}{2} \ln |x - \xi_j| (b_j, c_j).$$

Suppose that we have computed b_j, c_j , $1 \leq j \leq m$, using Remark 3.3 and thereby obtained $g_0 = \psi_0 + i\widehat{\psi}_0$ as in Proposition 3.2. Since g_0 has an antiderivative, we have that the vector fields

$$\mathbf{F}_0 = \begin{pmatrix} \psi_0 \\ -\widehat{\psi}_0 \end{pmatrix}, \quad \widehat{\mathbf{F}}_0 = \begin{pmatrix} \widehat{\psi}_0 \\ \psi_0 \end{pmatrix}$$

are conservative. Let $\rho_0, \widehat{\rho}_0$ be their corresponding potentials, then it follows from the Cauchy-Riemann equations that $\widehat{\rho}_0$ is a harmonic conjugate of ρ_0 , and their Neumann data is supplied with

$$\frac{\partial \rho_0}{\partial \mathbf{n}} = \mathbf{F}_0 \cdot \mathbf{n}, \quad \frac{\partial \widehat{\rho}_0}{\partial \mathbf{n}} = \widehat{\mathbf{F}}_0 \cdot \mathbf{n}.$$

The solution to the Neumann problem $\Delta\rho_0 = 0$, $\nabla\rho_0 \cdot \mathbf{n} = \mathbf{F}_0 \cdot \mathbf{n}$ is unique up to an additive constant, and similarly for $\widehat{\rho}_0$. Given the conclusion of Remark 2.2, we may fix these constants arbitrarily, and we make the choice to impose

$$\int_{\partial K} \rho_0 \, ds = 0, \quad \int_{\partial K} \widehat{\rho}_0 \, ds = 0.$$

Using the same techniques used to solve (8), we may determine the traces of $\rho, \widehat{\rho}$ by solving

$$(21) \quad \frac{1}{2} \rho_0(x) + \int_{\partial K} \left(\frac{\partial G(x, y)}{\partial \mathbf{n}(y)} + 1 \right) \rho_0(y) \, dS(y) = \int_{\partial K} G(x, y) \mathbf{F}_0(y) \cdot \mathbf{n}(y) \, dS(y),$$

$$(22) \quad \frac{1}{2} \widehat{\rho}_0(x) + \int_{\partial K} \left(\frac{\partial G(x, y)}{\partial \mathbf{n}(y)} + 1 \right) \widehat{\rho}_0(y) \, dS(y) = \int_{\partial K} G(x, y) \widehat{\mathbf{F}}_0(y) \cdot \mathbf{n}(y) \, dS(y).$$

In summary, we have the following recipe to determine an anti-Laplacian Φ of a given harmonic function ϕ on a multiply connected domain K :

- (a) Write $\phi = \psi + \sum_j a_j \lambda_j$ as in Theorem 3.1, and determine $\widehat{\psi}$ and a_1, \dots, a_m using (17) and (18).
- (b) Determine $b_1, \dots, b_m, c_1, \dots, c_m$ by computing (20).
- (c) Set

$$\psi_0 = \psi - \sum_{j=1}^m (b_j \mu_j - c_j \widehat{\mu}_j), \quad \widehat{\psi}_0 = \widehat{\psi} - \sum_{j=1}^m (c_j \mu_j + b_j \widehat{\mu}_j).$$

- (d) Solve (21) and (22) using $\mathbf{F}_0 = (\psi_0, -\widehat{\psi}_0)$ and $\widehat{\mathbf{F}}_0 = (\widehat{\psi}_0, \psi_0)$.
- (e) Set

$$\Phi(x) = \frac{1}{4} (x_1 \rho_0(x) + x_2 \widehat{\rho}_0(x)) + \sum_{j=1}^m M_j(x; b_j, c_j) + \sum_{j=1}^m a_j \Lambda_j(x).$$

3.3. Summary of Multiply Connected Case. The strategies outlined in Section 2 for expanding the H^1 semi-inner product and L^2 inner product and reducing each term to integrals along the boundary ∂K still hold in the multiply connected case. The two primary ways in which the computations have changed in the multiply connected case is (i) the Dirichlet-to-Neumann map for harmonic functions, and (ii) obtaining an anti-Laplacian of a harmonic function.

We also note that the FFT-based method (10) can still be used to obtain $\partial\widehat{\psi}/\partial\mathbf{t}$ from $\widehat{\psi}|_{\partial K}$, *but must be used on each component $\partial K_0, \partial K_1, \dots, \partial K_m$ of the boundary separately*. An astute reader may also notice that similar concerns would thwart our attempts to obtain $\rho_0, \widehat{\rho}_0$ with an FFT-based approach when K is multiply connected, in contrast to the simply connected case.

Should we wish to obtain interior values of

$$v(x) = \psi(x) + P(x) + \sum_{j=1}^m a_j \lambda_j(x),$$

which we emphasize is optional, we may proceed as follows. The values of P and λ_j may be obtained through direct computation. To see how to obtain interior values of ψ , consider the complex contour integral of $f = \psi + i\widehat{\psi}$ along the outer boundary ∂K_0 . Let γ be the positively oriented boundary of a closed disk that lies in K and is centered at a fixed $z \in K$. Then ∂K_0 can be decomposed into the chain

$$\partial K_0 \sim \gamma - \partial K_1 - \dots - \partial K_m$$

with the inner boundaries oriented clockwise. So integrating and applying Cauchy's integral formula to γ yields

$$\oint_{\partial K_0} \frac{f(\zeta)}{\zeta - z} \, d\zeta = 2\pi i f(z) - \sum_{j=1}^m \oint_{\partial K_j} \frac{f(\zeta)}{\zeta - z} \, d\zeta,$$

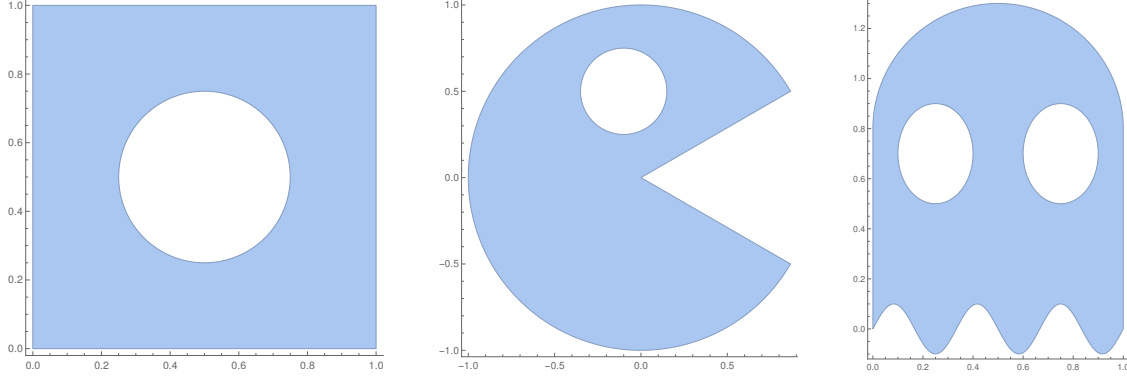


FIGURE 2. Punctured cells used for numerical experiments in Section 4.

and rearranging gives the familiar formula

$$f(z) = \frac{1}{2\pi i} \oint_{\partial K} \frac{f(\zeta)}{\zeta - z} d\zeta, \quad z \in K,$$

provided that we orient the boundary components properly. The same argument can be applied to show that the components of the gradient can be obtained in the interior by applying the above result to f' , and similarly for higher derivatives.

4. NUMERICAL EXAMPLES

For each of the following examples, we pick explicit functions $v, w \in H^1(K) \cap C^2(K)$ of the form

$$v = \phi + P, \quad w = \psi + Q,$$

where ϕ, ψ are harmonic functions and P, Q are polynomials. While we will pick v, w to be explicitly-defined, note that only the boundary traces $v|_{\partial K}, w|_{\partial K}$ and the coefficients of the polynomial Laplacians $\Delta v, \Delta w$ are supplied as input for the computations. Using explicitly defined functions is convenient for convergence studies, but in practice the computations will work the same for implicitly-defined functions.

Unless otherwise noted, we keep the Kress parameter $\sigma = 7$ fixed, as we observed that this value of the Kress parameter gave satisfactory results under a wide range of circumstances. Boundary integrals are evaluated by applying the trapezoid rule.

In each example, reference values for the H^1 and L^2 (semi-)inner products were obtained with *Wolfram Mathematica*. The mesh cell K was defined using `ImplicitRegion[]`, and volumetric integrals were computed using `NIntegrate[]`. We remark that our implementation, albeit far from optimized, was significantly faster than *Mathematica* for computing these kinds of integrals. (In fairness, we compute these integrals as boundary integrals, whereas it seems that *Mathematica* implements general-purpose adaptive 2D quadrature over the volume, so perhaps the comparison in performance is unjustified.) For each reference value, we also give the error estimate that was provided by *Mathematica*.

Each of the numerical examples in this section is presented with Jupyter Notebook in the GitHub repository

<https://github.com/samreynoldsmath/PuncturedFEM>

which also contains the Python source code implementing the numerical methods we have described in this work.

Example 4.1 (Punctured Square). Let $K_0 = (0, 1) \times (0, 1)$ be a unit square, and let $K_1 = \{x \in \mathbb{R}^2 : |x - \xi| < 1/16\}$ be a disk of radius $1/4$ centered at $\xi = (1/2, 1/2)$. The cell under consideration is the square with the disk removed, $K = K_0 \setminus \overline{K_1}$, as depicted in the left-hand side of Figure 2. Define

$$v(x) = e^{x_1} \cos x_2 + \ln |x - \xi| + x_1^3 x_2 + x_1 x_2^3.$$

TABLE 1. Errors in intermediate quantities for v on the square with a circular hole in Example 4.1: the logarithmic coefficient a_1 , the trace of the harmonic conjugate $\widehat{\psi}$, the weighted normal derivative wnd, and the trace of the anti-Laplacian Φ . The latter three are given in the L^2 boundary norm.

n	a_1 error	$\widehat{\psi}$ error	wnd error	Φ error
4	1.7045e-03	3.5785e-02	2.8201e-01	8.3234e-03
8	3.5531e-07	2.6597e-04	1.2855e-03	3.9429e-05
16	1.0027e-09	1.1884e-06	3.7415e-06	3.3785e-07
32	3.5905e-13	2.3095e-09	1.0434e-08	1.9430e-09
64	1.8874e-14	1.6313e-12	6.4780e-11	7.0728e-12

Notice that v can be decomposed into

$$v = \phi + P, \quad \phi(x) = e^{x_1} \cos x_2 + \ln|x - \xi|, \quad P(x) = x_1^3 x_2 + x_1 x_2^3,$$

with ϕ being harmonic and the polynomial P having the Laplacian

$$\Delta v(x) = \Delta P(x) = 12x_1 x_2.$$

Furthermore, ϕ can be decomposed as

$$\phi(x) = \psi(x) + a_1 \ln|x - \xi_1|$$

with $a_1 = 1$ and $\xi_1 = \xi = (1/2, 1/2)$. In Table 1, we report the errors in the computed approximations of a_1 , $\widehat{\psi}$, the weighted normal derivative (wnd) of ϕ , and the trace of the anti-Laplacian Φ . Since a harmonic conjugate $\widehat{\psi}$ is unique only up to an additive constant, we compute the error as

$$\left(\int_{\partial K} (\widehat{\psi}_{\text{exact}} - \widehat{\psi}_{\text{computed}} + c)^2 ds \right)^{1/2},$$

where c is a constant minimizing the $L^2(\partial K)$ distance between the traces of $\widehat{\psi}_{\text{exact}}$ and $\widehat{\psi}_{\text{computed}}$, namely

$$c = -\frac{1}{|\partial K|} \int_{\partial K} (\widehat{\psi}_{\text{exact}} - \widehat{\psi}_{\text{computed}}) ds.$$

In general, an anti-Laplacian Φ is unique only up to the addition of a harmonic function, which is much less restrictive. However, we see from Remark 2.2 that two different anti-Laplacians computed using the techniques described will differ by the addition of a linear function $c_1 x_1 + c_2 x_2$ for some constants c_1, c_2 . It follows that the difference between Φ_{computed} and

$$\Phi_{\text{exact}}(x) = \frac{1}{4} e^{x_1} (x_1 \cos x_2 + x_2 \sin x_2) + \frac{1}{4} |x - \xi|^2 (\ln|x - \xi| - 1)$$

ought to be well-modeled by $c_1 x_1 + c_2 x_2$, and we choose to determine optimal constants c_1, c_2 via least-squares. Upon doing so, we compute the error in Φ with

$$\left(\int_{\partial K} (\Phi_{\text{exact}} - \Phi_{\text{computed}} + c_1 x_1 + c_2 x_2)^2 ds \right)^{1/2}.$$

In Table 1, we list the absolute error in the logarithmic coefficient a_1 , as well as the L^2 boundary norm of the errors in the harmonic conjugate trace $\widehat{\psi}|_{\partial K}$, the weighted normal derivative of ϕ , and the trace of the anti-Laplacian Φ . We observe superlinear convergence in these quantities with respect to the boundary discretization parameter n . In Table 2, we provide the errors in the H^1 semi-inner product and L^2 inner product of v and w , where

$$w(x) = \frac{x_1 - 0.5}{(x_1 - 0.5)^2 + (y - 0.5)^2} + x_1^3 + x_1 x_2^2.$$

TABLE 2. Absolute errors in the H^1 semi-inner product and L^2 inner product for the Punctured Square (Example 4.1), Pac-Man (Example 4.2), and Ghost (Example 4.3).

n	Punctured Square		Pac-Man		Ghost	
	H^1 error	L^2 error	H^1 error	L^2 error	H^1 error	L^2 error
4	1.5180e-02	3.4040e-03	7.2078e-02	2.1955e-02	2.4336e+00	5.9408e-03
8	2.6758e-04	8.3812e-05	3.3022e-02	5.4798e-03	1.0269e-02	1.3086e-02
16	8.4860e-07	3.8993e-08	1.2495e-03	1.0159e-04	1.5273e-03	1.3783e-04
32	1.0860e-09	2.8398e-11	6.5683e-06	4.6050e-07	5.3219e-07	8.1747e-07
64	9.5390e-13	1.1036e-13	4.6834e-08	2.1726e-09	1.5430e-11	4.6189e-11

The reference values

$$\int_K \nabla v \cdot \nabla w \, dx \approx 4.46481780319135 \pm 9.9241 \times 10^{-15} ,$$

$$\int_K v w \, dx \approx 1.39484950156676 \pm 2.7256 \times 10^{-16}$$

were obtained with *Mathematica*, as noted above. Notice that the convergence trends in these quantities parallels those of the intermediate quantities found in Table 1.

Example 4.2 (Pac-Man). For our next example, we consider the Pac-Man domain $K = K_0 \setminus \overline{K_1}$, where K_0 is the sector of the unit circle centered at the origin for $\theta_0 < \theta < 2\pi - \theta_0$, $\theta_0 = \pi/6$, and K_1 is a disk of radius $1/4$ centered at $(-1/10, 1/2)$. (See Figure 2, center.) The function

$$v(x) = r^\alpha \sin(\alpha\theta)$$

specified in polar coordinates (r, θ) is harmonic everywhere except possibly the origin for any fixed $\alpha > 0$. For the choice $0 < \alpha < 1$, we have that the gradient of v is unbounded near the origin; indeed, $|\nabla v| = \alpha r^{\alpha-1}$. Noting that the boundary ∂K intersects the origin, it follows that normal derivative of v is also unbounded near the origin. To test whether our strategy is viable for such functions, we compute the H^1 seminorm and L^2 norm of v for $\alpha = 1/2$. The results are given in Table 2, using the reference values

$$\int_K |\nabla v|^2 \, dx \approx 1.20953682240855912 \pm 2.3929 \times 10^{-18} ,$$

$$\int_K v^2 \, dx \approx 0.97793431492143971 \pm 3.6199 \times 10^{-19} .$$

Although convergence is still rapid in this case, it is less so than in the previous example, as may be expected when considering more challenging integrands, as we have here.

Example 4.3 (Ghost). Our final example demonstrates that our method works when K has more than one puncture, as well as when the boundary has edges that are not line segments or circular arcs. The lower edge of the Ghost is the sinusoid $x_2 = 0.1 \sin(6\pi x_1)$ for $0 < x_1 < 1$, the sides are vertical line segments, the upper boundary is a circular arc of radius $1/2$ centered at $(0.5, 0.8)$, and the inner boundaries are ellipses with 0.15 and 0.2 as the semi-minor and semi-major axes, respectively, with one centered at $(0.25, 0.7)$ and the other at $(0.75, 0.7)$. (See Figure 2, right.) The functions we choose to integrate are

$$v(x) = \frac{x_1 - 0.25}{(x_1 - 0.25)^2 + (x_2 - 0.7)^2} + x_1^3 x_2 + x_2^2 ,$$

$$w(x) = \ln [(x_1 - 0.75)^2 + (x_2 - 0.7)^2] + x_1^2 x_2^2 - x_1 x_2^3 .$$

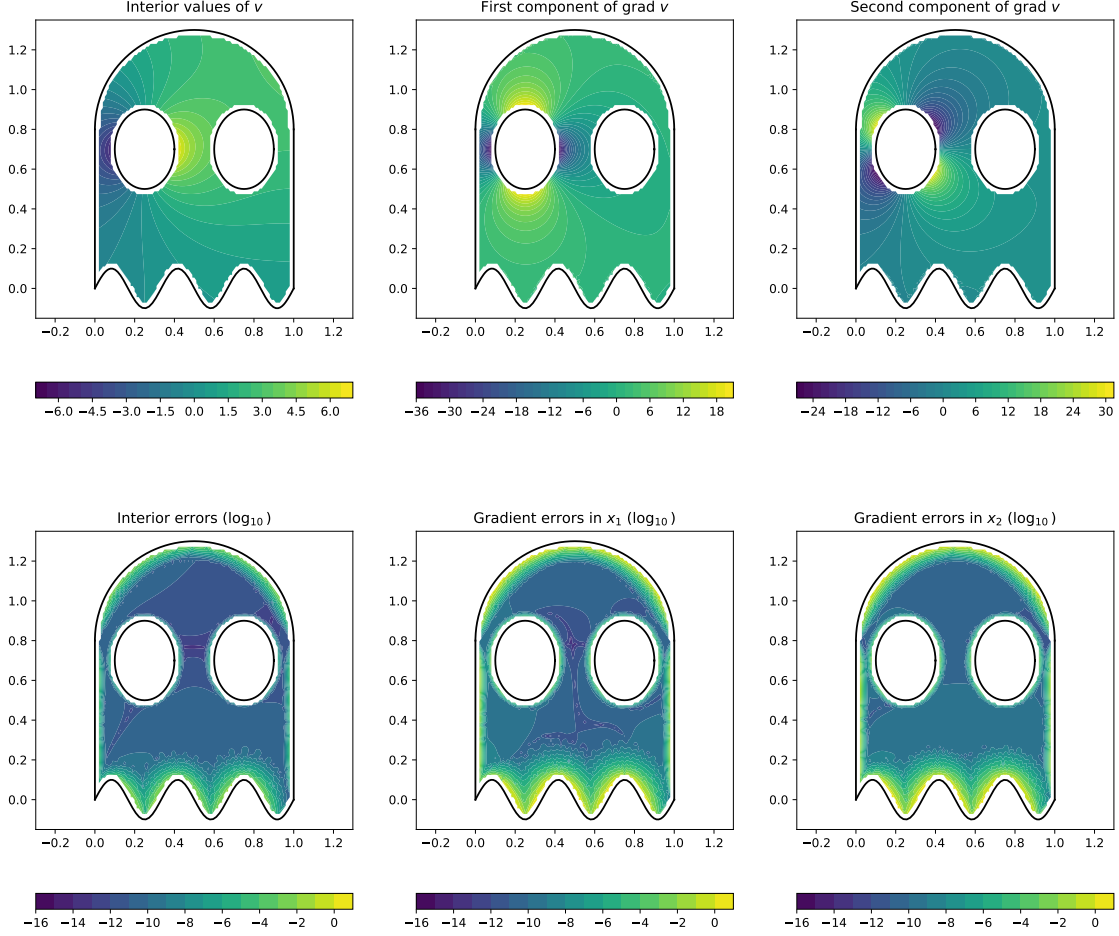


FIGURE 3. Interior values of v and ∇v in Example 4.3. In the left column, we have the computed values of v on top, and the base 10 logarithm of the absolute error on bottom. This setup is repeated in the middle and right columns for the components of the gradient.

Notice that these functions have singularities in the holes of K , one rational and the other logarithmic. In Table 2, we compare the computed H^1 and L^2 (semi-)inner products to the reference values

$$\int_K \nabla v \cdot \nabla w \, dx \approx -6.311053612386 \pm 3.6161 \times 10^{-12} ,$$

$$\int_K v w \, dx \approx -3.277578636852 \pm 1.0856 \times 10^{-13} .$$

We conjecture that for $n = 4$, the error in the H^1 semi-inner product is significantly worse than in the other two examples because this level of boundary discretization is insufficient to fully capture the oscillatory behavior of the lower edge.

Lastly, we demonstrate the ability to obtain interior values of v and ∇v in the interior of K in Figure 3. All computations used to generate these values used the boundary discretization parameter $n = 64$. Due to the factor(s) of $\zeta - z$ in the denominator of the integrand in Cauchy's integral formula, where ζ is a point on the boundary and z is the point in the interior where we wish to evaluate v , notice that the error in evaluation is considerably greater when z is near the boundary. For this reason, we choose to not to perform the evaluation if $|\zeta - z| < \varepsilon$ is found to hold for some boundary point $\zeta \in \partial K$ and a fixed $\varepsilon > 0$. For this example, we chose $\varepsilon = 0.02$.

5. CONCLUSION

We have seen that, given implicitly-defined functions v, w of the type that arise in a finite element setting, we can efficiently compute the H^1 semi-inner product and L^2 inner product of v and w over multiply connected curvilinear mesh cells. All of the necessary computations occur only on the boundary of mesh cells, although we have the option of obtaining interior values of these functions and their derivatives using quantities obtained in the course of these calculations. Two key computations needed for our approach are (i) a Dirichlet-to-Neumann map for harmonic functions, and (ii) finding the trace and normal derivative of an anti-Laplacian of a harmonic function. We have described how both of these computations may be feasibly accomplished on planar curvilinear mesh cells with holes. Numerical examples demonstrate superlinear convergence with respect to the number of sampled boundary points.

FUNDING

This work was partially supported by the National Science Foundation through NSF grant DMS-2012285 and NSF RTG grant DMS-2136228.

CODE AVAILABILITY

Python code used for the experiments in this manuscript is publicly available at <https://github.com/samreynoldsmath/PuncturedFEM>

REFERENCES

- [1] F. Aldakheel, B. Hudobivnik, E. Artioli, L. Beirão da Veiga, and P. Wriggers. Curvilinear virtual elements for contact mechanics. *Comput. Methods Appl. Mech. Engrg.*, 372:113394, 19, 2020.
- [2] A. Anand, J. S. Owall, S. E. Reynolds, and S. Weißer. Trefftz Finite Elements on Curvilinear Polygons. *SIAM J. Sci. Comput.*, 42(2):A1289–A1316, 2020.
- [3] P. F. Antonietti, P. Houston, and G. Pennesi. Fast numerical integration on polytopic meshes with applications to discontinuous Galerkin finite element methods. *J. Sci. Comput.*, 77(3):1339–1370, 2018.
- [4] S. Axler. Harmonic functions from a complex analysis viewpoint. *Amer. Math. Monthly*, 93(4):246–258, 1986.
- [5] L. Beirão da Veiga, F. Brezzi, L. D. Marini, and A. Russo. Polynomial preserving virtual elements with curved edges. *Math. Models Methods Appl. Sci.*, 30(8):1555–1590, 2020.
- [6] L. Beirão da Veiga, A. Russo, and G. Vacca. The virtual element method with curved edges. *ESAIM Math. Model. Numer. Anal.*, 53(2):375–404, 2019.
- [7] L. Beirão da Veiga, F. Brezzi, A. Cangiani, G. Manzini, L. D. Marini, and A. Russo. Basic principles of virtual element methods. *Math. Models Methods Appl. Sci.*, 23(1):199–214, 2013.
- [8] L. Beirão da Veiga, F. Brezzi, L. D. Marini, and A. Russo. The hitchhiker’s guide to the virtual element method. *Math. Models Methods Appl. Sci.*, 24(8):1541–1573, 2014.
- [9] F. Brezzi and L. D. Marini. Virtual element and discontinuous Galerkin methods. In *Recent developments in discontinuous Galerkin finite element methods for partial differential equations*, volume 157 of *IMA Vol. Math. Appl.*, pages 209–221. Springer, Cham, 2014.
- [10] D. Copeland, U. Langer, and D. Pusch. From the boundary element domain decomposition methods to local Trefftz finite element methods on polyhedral meshes. In *Domain decomposition methods in science and engineering XVIII*, volume 70 of *Lect. Notes Comput. Sci. Eng.*, pages 315–322. Springer, Berlin, 2009.
- [11] F. Dassi, A. Fumagalli, D. Losapio, S. Scialò, A. Scotti, and G. Vacca. The mixed virtual element method on curved edges in two dimensions. *Comput. Methods Appl. Mech. Engrg.*, 386:Paper No. 114098, 25, 2021.
- [12] P. R. Garabedian. *Partial Differential Equations*. John Wiley & Sons, New York, 1964.
- [13] A. Greenbaum, L. Greengard, and G. B. McFadden. Laplace’s equation and the Dirichlet-to-Neumann map in multiply connected domains. *Journal of Computational Physics*, 105(1):267–278, 1993.
- [14] W. Hackbusch. *Hierarchical matrices: algorithms and analysis*, volume 49 of *Springer Series in Computational Mathematics*. Springer, Heidelberg, 2015.
- [15] H. Hakula. Resolving boundary layers with harmonic extension finite elements. *Mathematical and Computational Applications*, 27(4), 2022.
- [16] C. Hofreither. L_2 error estimates for a nonstandard finite element method on polyhedral meshes. *J. Numer. Math.*, 19(1):27–39, 2011.
- [17] C. Hofreither, U. Langer, and C. Pechstein. Analysis of a non-standard finite element method based on boundary integral operators. *Electron. Trans. Numer. Anal.*, 37:413–436, 2010.
- [18] C. Hofreither, U. Langer, and S. Weißer. Convection-adapted BEM-based FEM. *ZAMM Z. Angew. Math. Mech.*, 96(12):1467–1481, 2016.
- [19] V. V. Karachik and N. A. Antropova. On the solution of a nonhomogeneous polyharmonic equation and the nonhomogeneous Helmholtz equation. *Differ. Uravn.*, 46(3):384–395, 2010.

- [20] R. Kress. A Nyström method for boundary integral equations in domains with corners. *Numer. Math.*, 58(2):145–161, 1990.
- [21] S. Lang. *Complex analysis*, volume 103 of *Graduate Texts in Mathematics*. Springer-Verlag, New York, fourth edition, 1999.
- [22] J. S. Ovall and S. E. Reynolds. A high-order method for evaluating derivatives of harmonic functions in planar domains. *SIAM J. Sci. Comput.*, 40(3):A1915–A1935, 2018.
- [23] J. S. Ovall and S. E. Reynolds. Quadrature for implicitly-defined finite element functions on curvilinear polygons. *Computers & Mathematics with Applications*, 107:1–16, 2022.
- [24] S. Weißer. Residual error estimate for bem-based fem on polygonal meshes. *Numer. Math.*, 118:765–788, 2011. 10.1007/s00211-011-0371-6.
- [25] S. Weißer. Arbitrary order Trefftz-like basis functions on polygonal meshes and realization in BEM-based FEM. *Comput. Math. Appl.*, 67(7):1390–1406, 2014.
- [26] S. Weißer. Residual based error estimate and quasi-interpolation on polygonal meshes for high order BEM-based FEM. *Comput. Math. Appl.*, 73(2):187–202, 2017.
- [27] S. Weißer. Anisotropic polygonal and polyhedral discretizations in finite element analysis. *ESAIM Math. Model. Numer. Anal.*, 53(2):475–501, 2019.
- [28] S. Weißer. *BEM-based Finite Element Approaches on Polytopal Meshes*, volume 130 of *Lecture Notes in Computational Science and Engineering*. Springer International Publishing, 1 edition, 2019.
- [29] S. Weißer and T. Wick. The dual-weighted residual estimator realized on polygonal meshes. *Comput. Methods Appl. Math.*, 18(4):753–776, 2018.
- [30] P. Wriggers, B. Hudobivnik, and F. Aldakheel. A virtual element formulation for general element shapes. *Comput. Mech.*, 66(4):963–977, 2020.
- [31] J. Xia, S. Chandrasekaran, M. Gu, and X. S. Li. Fast algorithms for hierarchically semiseparable matrices. *Numer. Linear Algebra Appl.*, 17(6):953–976, 2010.

JEFFREY S. OVALL, FARIBORZ MASEEH DEPARTMENT OF MATHEMATICS AND STATISTICS, PORTLAND STATE UNIVERSITY, PORTLAND, OR 97201
Email address: jovall@pdx.edu

SAMUEL REYNOLDS, FARIBORZ MASEEH DEPARTMENT OF MATHEMATICS AND STATISTICS, PORTLAND STATE UNIVERSITY, PORTLAND, OR 97201
Email address: ser6@pdx.edu